

Doped holes and Mn valence in manganites: a polarized soft x-ray absorption study of  $\text{LaMnO}_3$  and quasi-2D manganite systems

This article has been downloaded from IOPscience. Please scroll down to see the full text article.

2008 J. Phys.: Condens. Matter 20 055215

(<http://iopscience.iop.org/0953-8984/20/5/055215>)

View [the table of contents for this issue](#), or go to the [journal homepage](#) for more

Download details:

IP Address: 129.252.86.83

The article was downloaded on 29/05/2010 at 08:06

Please note that [terms and conditions apply](#).

# Doped holes and Mn valence in manganites: a polarized soft x-ray absorption study of $\text{LaMnO}_3$ and quasi-2D manganite systems

K B Garg<sup>1,8</sup>, N L Saini<sup>2</sup>, B R Sekhar<sup>3</sup>, R K Singhal<sup>1</sup>, B Doyle<sup>4</sup>, S Nannarone<sup>4,5</sup>, F Bondino<sup>6</sup>, E Magnano<sup>6</sup>, E Carleschi<sup>6</sup> and T Chatterji<sup>7</sup>

<sup>1</sup> Department of Physics, University of Rajasthan, Jaipur-302004, India

<sup>2</sup> Dipartimento di Fisica, Università di Roma 'La Sapienza', Piazzale Aldo Moro 2, 00185 Roma, Italy

<sup>3</sup> Institute of Physics, Sachivalaya Marg, Bhubaneswar-751005, India

<sup>4</sup> Laboratorio Nazionale TASC, INFN-CNR, S. S. 14, km 163.5, Area Science Park, 34012 Basovizza (TS), Italy

<sup>5</sup> Dipartimento di Ingegneria dei Materiali e dell'Ambiente, Università di Modena e Reggio Emilia, Via Vignolese 905, 41100 Modena, Italy

<sup>6</sup> CNR—Laboratorio Nazionale TASC-INFN, Area Science Park—Basovizza, Edificio MM—S. S. 14 km 163,5, I-34012 Basovizza (TS), Italy

<sup>7</sup> Science Division, Institut Laue-Langevin, BP 156, 38042 Grenoble Cedex 9, France

E-mail: [krish35@sancharnet.in](mailto:krish35@sancharnet.in) (K B Garg)

Received 1 October 2007, in final form 17 November 2007

Published 17 January 2008

Online at [stacks.iop.org/JPhysCM/20/055215](http://stacks.iop.org/JPhysCM/20/055215)

## Abstract

The question of Mn valence and symmetry and population of doped holes in  $\text{La}_{1.2}\text{Sr}_{1.65}\text{Ca}_{0.15}\text{Mn}_2\text{O}_7$  and  $\text{LaSr}_2\text{Mn}_2\text{O}_7$  bilayer single crystals has been studied with polarized soft x-ray absorption spectroscopy. The observed changes in the O K and Mn L spectra with polarization provide a strong indication for the existence of a competition between the charge dynamics and the lattice distortion that leads to transfer of some of the holes doped in the out-of-plane ( $3z^2 - r^2$ ) states to the in-plane ( $x^2 - y^2$ ) states. The changes observed in these with doping are shown not due to a decrease in the electron population in the  $d_{x^2-y^2}$  states but caused by an increase in density of holes in the  $d_{z^2-x^2}$  and  $d_{z^2-y^2}$  states, and the electrons predominantly occupy the corresponding orthogonal states, i.e.,  $d_{3x^2-r^2}$  and  $d_{3y^2-r^2}$ . No evidence is found for the existence of a formal  $\text{Mn}^{4+}$  valence state in these systems.

(Some figures in this article are in colour only in the electronic version)

## 1. Introduction

Hole doped manganites  $\text{R}_{1-x}\text{A}_x\text{MnO}_3$ , wherein R is rare-earth ion and A a divalent cation (Ca, Sr or Ba), have received great attention in recent times [1] for a variety of reasons. Strong correlation and lattice distortion in these materials lead to a complex and strong interplay amongst charge, spin, and orbital

degrees of freedom which, in turn, lead to exotic macroscopic effects like the colossal magnetoresistance (CMR) around the ferromagnetic transition temperature  $T_c$ . Besides, such a behaviour raises further fundamental questions in the field.

The basic physics of the hole doped manganites can be understood on the basis of interplay between strong Hund's rule coupling in Mn and the Jahn–Teller (JT) distortion of the  $\text{MnO}_6$  octahedron [2]. The divalent cation A in the doped manganites induces the  $\text{Mn}^{3+}$  ion to go over to a

<sup>8</sup> Author to whom any correspondence should be addressed.

mixture of  $\text{Mn}^{3+}$  and  $\text{Mn}^{4+}$  (all valences are nominal here). Double exchange between the  $\text{Mn}^{3+}$  and  $\text{Mn}^{4+}$  ions then drives the parent compound  $\text{LaMnO}_3$  characterized by an insulating antiferromagnetic ground state to a ferromagnetic metallic ground state for  $x \geq 0.2$  in the doped state. Several models [3]—based on the double-exchange (DE) interaction, Jahn–Teller distortion, antiferromagnetic (AF) superexchange, charge–orbital ordering interaction, phase separation, etc, have been proposed to account for some of the exotic properties observed in manganites.

With the recent success at synthesis, the bilayer manganites,  $\text{La}_{2-2x}\text{Sr}_{1+2x}\text{Mn}_2\text{O}_7$ , have attracted a great deal of attention of researchers because of their exotic electrical and magnetic properties [4]. Interesting results have been reported on the  $n = 2$  compounds of the Ruddlesden–Popper series generally described as  $(\text{Ln}_{1-x}\text{A}_x)_{n+1}\text{Mn}_n\text{O}_{3n+1}$ . In the  $n = 2$  bilayer Mn perovskite, two  $\text{MnO}_6$  layers are alternately stacked with  $(\text{Ln}, \text{A})_2\text{O}_2$  layers along the  $c$  axis of the structure whereas in the case of cubic  $\text{Ln}_{1-x}\text{A}_x\text{MnO}_3$  the  $\text{MnO}_6$  octahedra extend all over the space. The reduced dimensionality of the  $n = 2$  compounds has been shown to have interesting consequences on their physical properties. Thus, the compound  $\text{La}_{1.2}\text{Sr}_{1.8}\text{Mn}_2\text{O}_7$  (40% doped bilayer) exhibits a paramagnetic to ferromagnetic transition (PFT) at  $T_c \sim 125$  K, accompanied by a semiconductor to metal transition (SMT) and the CMR reaches 98% near  $T_c$  [4]. At room temperature, the Mn–O bonds are found to be longer in the  $z$  direction than in the  $x$ – $y$  plane. This would imply occupation of the  $3d_{z^2-r^2}$  orbital while the hybridization would favour the occupation of the  $3d_{x^2-y^2}$  one [5]. It thus offers a possibility of studying interplay between hybridization and chemical potential.

The 50% doped bilayer  $\text{LaSr}_2\text{Mn}_2\text{O}_7$  however shows very different properties. It has equal numbers of  $e_g$  electrons and holes in the valence band. It does not show any PFT or SMT transition. Instead it shows a long-range charge and orbital (CO) order [6]. The CO order observed at  $x = 0.5$  is commonly referred to as ‘zigzag,’ ‘checkerboard,’ or ‘CE’ due to early predictions by Goodenough that the CE–AF spin ordering would be favoured by a specific charge–orbital configuration comprised of a checkerboard arrangement of  $\text{Mn}^{3+}$  and  $\text{Mn}^{4+}$  sites that hosts diagonal zigzag chains of occupied  $d(3z^2 - r^2)$  orbitals [7]. Experimental evidence for this connection has been provided by x-ray and neutron diffraction experiments [8].

The  $\text{LaSr}_2\text{Mn}_2\text{O}_7$  bilayer resistivity shows a significant increase at the CO ordering temperature,  $T_{\text{CO}} \sim 210$  K, involving the localization of the  $e_g$  charge carriers and a cooperative structural distortion [7, 8]. At decreasing temperatures, however, this trend is soon arrested by the onset of A-type AF order at  $T_{N(\text{A})} \sim 170$  K. The A–AF phase continues to grow and eventually results in the re-entrant disappearance of CO order, accompanied by a drop in the resistivity. Recent theoretical efforts suggest that the A-type phase exhibits  $x^2 - y^2$  orbital order, while also being a double-exchange metal so that the carriers are delocalized, but restrict themselves to the preferred orbitals as they traverse the lattice. This effect has been referred

to as orbital polarization [9]. While diffraction studies have uncovered no evidence of the breathing-mode distortions [10] that would arise in a charge-ordered  $x^2 - y^2$  orbital lattice, a series of resonant x-ray scattering studies [11] support the existence of  $x^2 - y^2$  orbital polarization in a charge-disordered A–AF state. The increased hopping within a double-exchange-dominated ferromagnetic sheet would provide for better electron transport than the CO state, though the AF coupling between sheets inhibits intersheet hopping. Results from electron diffraction experiments [6] have also been shown to point to  $d_{3x^2-r^2}/d_{3y^2-r^2}$  orbital ordering of  $\text{Mn}^{3+}$  accompanying the real-space ordering of 1:1  $\text{Mn}^{3+}/\text{Mn}^{4+}$  species.

Two of the key attributes that control the properties of doped manganites are: the symmetry of the doped holes and the valence(s) of the Mn ion and which thus deserve due attention. While there is almost complete unanimity on the former the same is not true about the latter. Frequently one uses the representation  $\text{Mn}^{3+}$  and  $\text{Mn}^{4+}$  for the Mn ion in one’s discussion but do the doped systems really have two species (in respect of valence) of the Mn ion,  $\text{Mn}^{3+}$  ( $3d^4$ ) and  $\text{Mn}^{4+}$  ( $3d^3$ ) in the lattice? X-ray absorption (XAS) is regarded as the most potent technique in respect of study of valence—it is well known that the absorption edge shifts to higher energy by  $\sim 1$ – $2$  eV as the valence of the absorbing ion increases by one—and is therefore ideally suited to answer the present question. However, there is lack of consensus even in interpretation of the XAS spectra in case of manganites. While some conclude the distinct presence of  $\text{Mn}^{2+}/\text{Mn}^{3+}/\text{Mn}^{4+}$  ions [12], for example whereas others dispute the very presence of two distinct valences species of Mn in the lattice (for example, [13, 14]). We have, therefore, attempted a probe on the twin aspects of symmetry of doped holes and valence of the Mn ions by making polarized O K and Mn L absorption measurements on 40% and 50% doped  $\text{La}_{1.2}\text{Sr}_{1.65}\text{Ca}_{0.15}\text{Mn}_2\text{O}_7$  and  $\text{LaSr}_2\text{Mn}_2\text{O}_7$  single crystals. We have also included an undoped  $\text{LaMnO}_3$  single crystal in our measurements for the sake of comparison. We have, thus, studied the doping as well as orientation dependence,  $E \parallel ab$  and  $E \parallel c$ , of the doped holes and Mn valence in these systems.

## 2. Experimental details

The single crystals were grown by the floating zone method in a mirror furnace. Magnetization and transport measurements on this crystal showed the transition temperatures  $T_c$  to be  $\sim 128$  K. Details of the sample preparation, characterization studies are published elsewhere [15]. Room temperature polarized XAS measurements were performed using the BEAR [16] and BACH [17] beamlines associated with ELETTRA at Trieste, Italy. At the BEAR beamline, the monochromatized radiation comes from a bending magnet, while at the BACH beamline it comes from an undulator. The resolution at the BEAR beamline at the O K edge was  $\sim 0.2$  eV while at the BACH beamline it was  $< 0.2$  eV. The Mn L and O K edge spectra were measured in both fluorescence (FY) and total yield detection (TY) mode on freshly prepared surfaces of the single crystals, obtained by *in situ* scraping of crystal faces

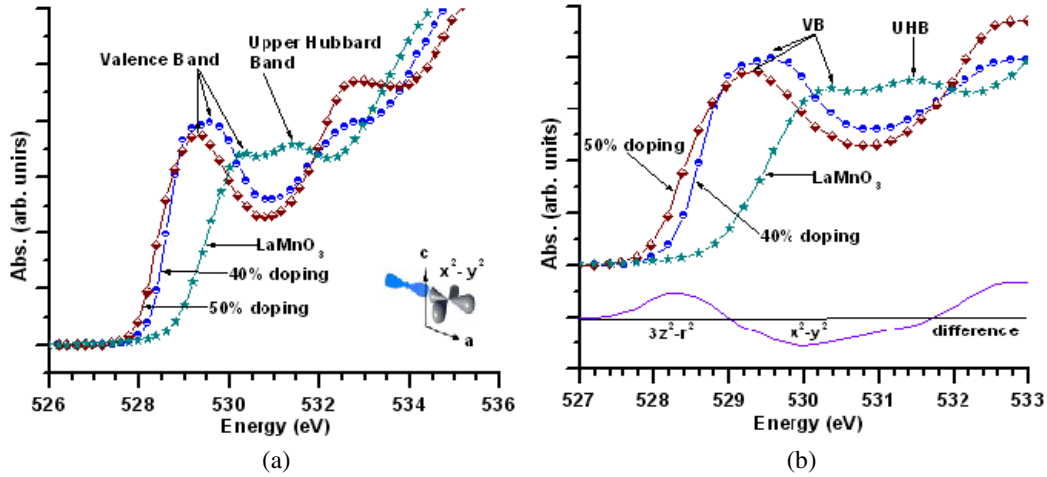


**Figure 1.** (a) The  $E \parallel ab$  polarized O K edge spectra from the undoped  $\text{LaMnO}_3$ , the 40% doped  $\text{La}_{1.2}\text{Sr}_{1.65}\text{Ca}_{0.15}\text{Mn}_2\text{O}_7$ , and the 50% doped  $\text{LaSr}_2\text{Mn}_2\text{O}_7$  crystal. (b) The pre-edge region from the spectra in (a) and the difference curve that represents the change in spectral weight as the level of doping is increased from 40% in  $\text{La}_{1.2}\text{Sr}_{1.65}\text{Ca}_{0.15}\text{Mn}_2\text{O}_7$  to 50% in the  $\text{LaSr}_2\text{Mn}_2\text{O}_7$  crystal.

inside the UHV chamber ( $1.0 \times 10^{-10}$  mbar) using a diamond file. The *in situ* scraping is repeated during the measurements to obtain a fresh surface as ‘dirty’ oxygen and carbon tend to get deposited on it with extended use. These are monitored by recording the O 1s and C 1s core level photoemission. As TY mode is surface-sensitive (penetration depth  $< 100$  Å) only FY (penetration depth  $\sim 1000$  Å at these energies) detected O K spectra are shown and these are duly corrected for self-absorption [18]. However, the Mn L spectra shown here are those recorded in the TY mode as the corresponding FY mode spectra tend to be get substantially distorted by self-absorption owing to the high absorption coefficient of Mn.

### 3. Results and discussion

Figures 1(a) and (b) respectively show the  $E \parallel ab$  polarized O K edge spectra and their pre-edge region obtained from the undoped  $\text{LaMnO}_3$ , the 40% doped  $\text{La}_{1.2}\text{Sr}_{1.65}\text{Ca}_{0.15}\text{Mn}_2\text{O}_7$ , and the 50% doped  $\text{LaSr}_2\text{Mn}_2\text{O}_7$  single crystals. Our spectra look very similar to those reported earlier [18–20]. Although the transition involves oxygen orbitals, the threshold structure observed at the oxygen K edge is determined by the electronic structure of the 3d-transition-metal ion [21]. Thus the XAS intensity at the oxygen K edge threshold region directly relates to both the hybridization of oxygen 2p with Mn 3d orbitals on the one hand and the availability of  $e_g$  character oxygen 2p orbitals on the other. The 3d transition metal is important because the oxygen 2p shell is full in an ionic picture. Empty oxygen 2p orbitals are created through ground-state hybridization between 3d-transition-metal orbitals and oxygen 2p orbitals.

The O K edge has a proven ability for studying the site symmetry and concentration of doped holes in as much as the pre-edge peaks in it make an appearance only when the system (perovskite) is doped with holes. Confining attention to the region of main interest ( $\sim 528$ – $532$  eV), the so-called pre-edge region, it can be seen that the first feature

comprises of two peaks. Following Merz *et al* [23], the peaks have been designated valence band (VB) and upper Hubbard band (UHB). The spectra, particularly the pre-edge region in figure 1(b), clearly show that doping leads to transfer of spectral weight from the UHB to VB and also how the latter tends to shift to lower energy. The VB shifts from  $\sim 530.2$  eV in  $\text{LaMnO}_3$  to  $\sim 529.5$  eV in the 50% doped  $\text{LaSr}_2\text{Mn}_2\text{O}_7$  system. Moreover, the UHB has a substantial intensity in  $\text{LaMnO}_3$  but loses almost all of it as the doping reaches near 50%. We would revert to this aspect a little later.

The O K and Mn L spectra in the manganites can perhaps be better understood by referring to the schematic diagram in figure 2. The metal sites in most manganites have octahedral site symmetry ( $O_h$ ) with each Mn ion surrounded by six oxygen ions to form the  $\text{MnO}_6$  octahedron. The Mn 3d orbital ion splits into triply degenerate  $t_{2g}$  and doubly degenerate  $e_g$  orbitals. In case of the quasi-two-dimensional bilayer manganite systems however, the site symmetry of the Mn ion is tetrahedral ( $D_{4h}$ ) due to lattice distortion, the in-plane Mn–O bonds get shortened and the out-of-plane Mn–O bonds elongated [20]. As a result, the degeneracy is lifted and the  $e_g$  orbital energy splits into in-plane orbital energy  $x^2 - y^2$  and out-of-plane  $3z^2 - r^2$  one. The  $t_{2g}$  energy likewise splits into the in-plane orbital energy  $xy$  and doubly degenerate out-of-plane  $xz, yz$  one. All this implies, therefore, that the ionic state of the parent Mn being  $3+ (d^4)$ , the doped holes would preferentially go to the out-of-plane  $3z^2 - r^2$  energy level of the  $e_g$  orbital. The spin configuration  $t_{2g}^3 e_g^1$  is due to Hund’s rule. The  $e_g$  occupation stays in the out-of-plane  $e_g$  orbital ( $3z^2 - r^2$ ), energetically lowered by the tetragonal distortion. Thus the doped hole is constrained to go only to the out-of-plane ( $3z^2 - r^2$ ) orbital and the in-plane  $x^2 - y^2$  state remains totally empty.

The near- $E_F$  region of the  $E \parallel a$  O K edge spectra in them would therefore be dominated by the unoccupied O orbitals that are  $\sigma$ -bonded to Mn  $3d_{z^2-r^2}$  and Mn  $3d_{x^2-y^2}$  states. The  $E \parallel a$  contribution would come from the orbital  $2p_x$  of the in-plane oxygen O(1), and the  $E \parallel b$  (equivalent to  $E \parallel a$  from symmetry conditions) from the O(1)  $2p_y$  state. Likewise, it is

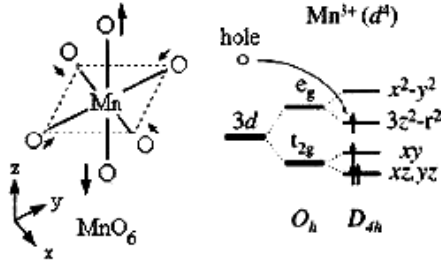


**Figure 2.** A schematic representation of the tetragonal distortion of the  $\text{MnO}_6$  octahedron (left side) and splitting of the energy of the Mn 3d orbital by the octahedral ( $O_h$ ) site symmetry (as in cubic manganites LSMO) and lifting of the degeneracy of  $e_g$  and  $t_{2g}$  orbitals due to the tetrahedral distortion ( $D_{4h}$ ) of the octahedron (as in quasi-two-dimensional bilayer systems).

the O  $2p_z$  orbitals of the apical oxygen that would provide the predominant contribution to the  $E \parallel c$  spectrum. The UHB (see figure 1) may thus be said to owe its spectral weight to  $\sigma$ -type hybridization of the O(1)  $2p_x$  and O(1)  $2p_y$  orbitals with the Mn 3d  $e_g$  states. It has a high intensity when the  $e_g$  state is half-filled (as in  $\text{LaMnO}_3$ ) which disappears when the  $e_g$  state is empty (as in the 50% doped crystal). Above assignment for the UHB is further supported by the observed doping dependent transfer of the spectral weight from it to the VB. This is easily seen by comparing the  $\text{LaMnO}_3$  spectrum with those for the doped crystals in the UHB region in figure 1(b)—the spectral weight in this region gets very strongly suppressed with doping. It is well known how the UHB loses its entire spectral weight in the  $E \parallel a$  polarized spectra for 50% doped systems in the quasi-2D systems [23]. A logical corollary of the above scheme would imply that all spectral weight in the pre-edge region for  $\text{LaMnO}_3$  must be confined to the UHB and none to the VB. However, the observed spectra for  $\text{LaMnO}_3$  (see figure 1) show comparable intensities for the UHB and VB. This is possible only if neither of the  $e_g$  orbitals, ( $x^2 - y^2$ ) and ( $3z^2 - r^2$ ), is completely empty which, in turn, would imply that the two must share the one electron that is available to the  $e_g$  state. For this to come about, some holes must reside on out-of-plane ( $3z^2 - r^2$ ) states, moving this band away from half-filling. Some of the holes doped in the out-of-plane ( $3z^2 - r^2$ ) states are transferred to the in-plane ( $x^2 - y^2$ ) as a consequence of competition between the charge dynamics and the lattice distortion [18]. The assignment of the first two loops in the difference spectrum in figure 1(b) to ( $3z^2 - r^2$ ) and ( $x^2 - y^2$ ) respectively is based on this premise.

Figure 3 compares the  $E \parallel a$  and  $E \parallel c$  spectra in case of the 40% doped crystal  $\text{La}_{1.2}\text{Sr}_{1.65}\text{Ca}_{0.15}\text{Mn}_2\text{O}_7$ . In figure 3(a) the  $E \parallel c$  spectrum is superposed on the  $E \parallel a$  for the 40% doped bilayer to show the difference. It also serves to illustrate that the  $E \parallel c$  spectrum arises mainly from transitions to the O(2)  $2p_z$  orbitals hybridized with Mn  $3d_{3z^2-r^2}$  states. The difference in the two spectra can be more clearly seen in figure 3(b). The difference spectrum is plotted by subtracting the  $E \parallel a$  spectrum from the  $E \parallel c$ . Our spectra are similar to those reported earlier in  $\text{La}_{1.2}\text{Sr}_{1.8}\text{Mn}_2\text{O}_7$  [18] and in  $\text{La}_{1-x}\text{Sr}_{1+x}\text{Mn}_1\text{O}_4$  [23]. Again, as in figure 1(b), the spectral

weight in the first two loops in the difference spectrum are respectively assigned to ( $3z^2 - r^2$ ) and ( $x^2 - y^2$ ) symmetry.

Also, the  $E \parallel c$  spectrum, unlike the  $E \parallel a$  case, appears to have a non-zero intensity in the UHB region. This is easily seen by the presence of the third small loop in the difference spectrum in figure 3(b). This, in turn, implies a decreasing but non-vanishing electron population in the  $3d_{3z^2-r^2}$  state. The  $E \parallel c$  spectrum differs from the  $E \parallel a$  one in yet another aspect. The VB in the former is a double-peak structure. This is manifest in the shape of the second loop in the difference spectrum in the beginning part wherein it shows a small kink. We have also seen the double-peak structure in the derivative spectrum as well as by fitting Lorentzian–Gaussian peaks to the spectrum. The double-peak structure would mean that the O(2)  $2p_z$  orbitals hybridize not only with the  $3d_{3z^2-r^2}$  states but also with another type of Mn 3d states that have out-of-plane contributions. Park *et al* [18] ascribe the double-peak structure to O(2)  $2p_z$  holes resulting from hybridization with the  $3z^2 - r^2$  and  $t_{2g}$  unoccupied states at low and high energies, respectively. These have, however, recently been identified as  $3d_{z^2-x^2}$  and  $3d_{z^2-y^2}$  states [23]. This would mean that the observed increase in intensity of the VB with doping in figure 1(b) is not caused by a decrease in the electron population in the Mn  $3d_{x^2-y^2}$  states but by an increase in density of holes in the  $3d_{z^2-x^2}$  and  $3d_{z^2-y^2}$  states.

We now turn attention to the Mn L spectra from these crystals. Figure 4 shows the  $E \parallel a$  polarized  $L_3$  spectrum from the crystals  $\text{LaMnO}_3$ , the 40% doped  $\text{La}_{1.2}\text{Sr}_{1.65}\text{Ca}_{0.15}\text{Mn}_2\text{O}_7$ , and the 50% doped  $\text{La}_{1.2}\text{Sr}_{1.8}\text{Mn}_2\text{O}_7$  crystal. The spectra were measured both in FY as well as TY modes. The FY detected Mn L spectra showed strong self-absorption effects influencing the relative intensities of the features, especially in respect of the  $L_2$  spectra. The FY and TY spectra were otherwise identical in respect of their fine structure. The spectra shown in figure 4 are those recorded using TY mode. The spectra look very similar to those reported by Abbate *et al* in the cubic  $\text{La}_{1-x}\text{Sr}_x\text{MnO}_3$  system [20] and Merz *et al* in the quasi-2d system  $\text{La}_{1-x}\text{Sr}_x\text{MnO}_4$  [23].

The spectra in figure 4 show the polarization dependence of the Mn  $L_3$  spectra in the 40% doped  $\text{La}_{1.2}\text{Sr}_{1.65}\text{Ca}_{0.15}\text{Mn}_2\text{O}_7$ , and the 50% doped  $\text{La}_{1.2}\text{Sr}_{1.8}\text{Mn}_2\text{O}_7$  bilayer systems. The spectra look different from each other, in case of the former (figure 4(a)), the feature A has a little more intensity in the  $E \parallel a$  spectrum as compared to that in the  $E \parallel c$  case for the 40% doped  $\text{La}_{1.2}\text{Sr}_{1.65}\text{Ca}_{0.15}\text{Mn}_2\text{O}_7$  system but the feature B shows exactly the opposite behaviour. This means that the holes/electrons must reside on different orbitals in the two cases. Also, the intensity of the Mn  $L_3$  edge, the initial rise, is noticeably higher in the  $E \parallel a$  polarization which means a higher density of holes in the  $3d_{x^2-y^2}$  states compared to the  $3d_{z^2-r^2}$  states.

Furthermore, the two polarized spectra turn out to be virtually identical in the 50% doped  $\text{LaSr}_2\text{Mn}_2\text{O}_7$  crystal which would imply that the holes must reside in this case on hybrid states that are symmetric with respect to the  $x$ - ( $y$ -) and  $z$ -axis. Also, the results for the O K edge must reflect in the Mn L spectra as well. In the discussion on the O K edge spectra we had emphasized that the  $3d_{x^2-y^2}$  orbitals of Mn hybridize



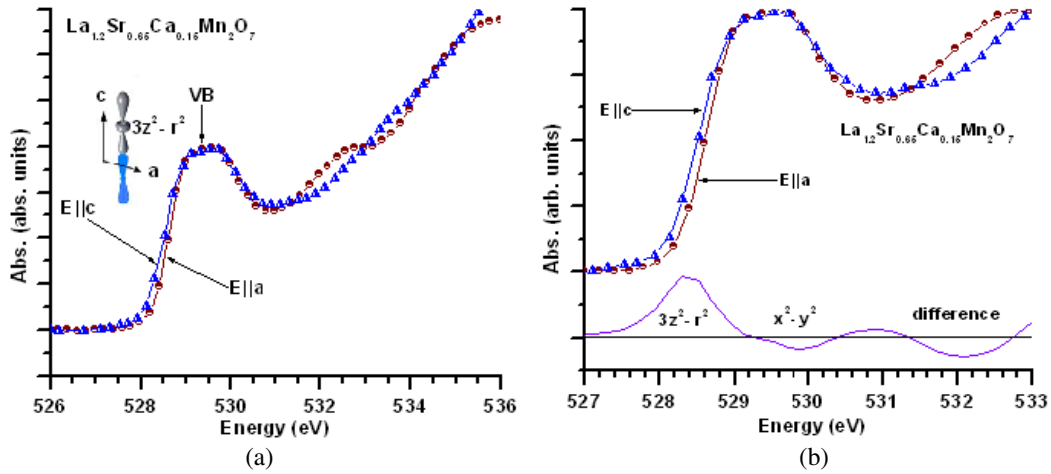


**Figure 3.** (a) Polarization dependence of the O K edge as seen from the  $E \parallel ab$  and  $E \parallel c$  spectra for the 40% doped bilayer  $\text{La}_{1.2}\text{Sr}_{1.65}\text{Ca}_{0.15}\text{Mn}_2\text{O}_7$ . (b) The pre-edge region from the spectra in (a) and the difference curve that represents the change in spectral weight as the polarization is changed from  $E \parallel c$  to  $E \parallel a$  in  $\text{La}_{1.2}\text{Sr}_{1.65}\text{Ca}_{0.15}\text{Mn}_2\text{O}_7$ .

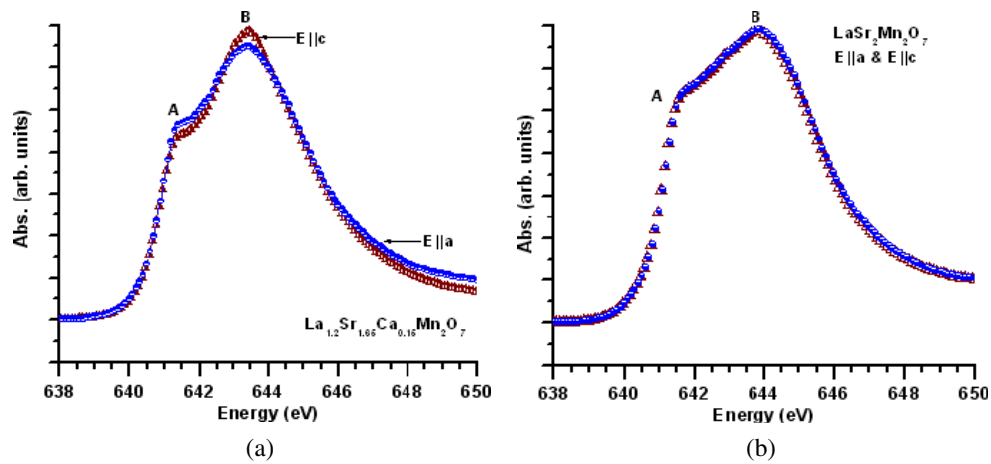


**Figure 4.** The  $E \parallel a$  (half-filled circles) and  $E \parallel c$  (half-filled triangles) polarized Mn  $L_3$  spectra for (a) the 40% doped  $\text{La}_{1.2}\text{Sr}_{1.65}\text{Ca}_{0.15}\text{Mn}_2\text{O}_7$ , and (b) the 50% doped  $\text{La}_{1.2}\text{Sr}_{1.8}\text{Mn}_2\text{O}_7$  crystals.

with the  $2p_x$  (or  $2p_y$ ) orbitals of in-plane O(1) whereas the Mn  $3d_{z^2-r^2}$  states hybridize with  $2p_z$  orbitals of the axial O(2). It is thus transitions from Mn  $2p$  to these hybridized  $3d$  states that would respectively yield the  $E \parallel a$  (or  $E \parallel b$ ) and the  $E \parallel c$  polarized  $L_3$  spectra of Mn. But, what states do the doped holes go to? To understand this let us first compare the  $E \parallel a$  polarized spectra for the  $\text{La}_{1.2}\text{Sr}_{1.65}\text{Ca}_{0.15}\text{Mn}_2\text{O}_7$  and the  $\text{La}_{1.2}\text{Sr}_{1.8}\text{Mn}_2\text{O}_7$  doped systems with  $\text{LaMnO}_3$  (figure 5).

From the three spectra shown in figure 5 it is easy to see that the Mn  $L_3$  multiplet in each of these cases has a feature that appears at energy of  $\sim 641.2$  eV (A) and an intensity maximum (B) that shows a progressive shift as the doping level increases from 0 to 50%. With the hole content increasing from 0% in  $\text{LaMnO}_3$  to 40% in  $\text{La}_{1.2}\text{Sr}_{1.8}\text{Mn}_2\text{O}_7$  and on to 50% in  $\text{LaSr}_2\text{Mn}_2\text{O}_7$ , the intensity of the  $L_3$  edge gets considerably reduced. Also, there is a small change in the shape of the multiplet with doping. The reduction in intensity of  $E \parallel a$  spectrum despite an increase in hole density (with doping) clearly indicates that hole doping must lead to

a transfer of electrons from out-of-plane states to orbitals with finite in-plane contributions. The Mn  $2p$  spectra thus support the conclusion derived from the O  $1s$  spectra earlier that the observed changes in intensity with doping is not caused by a decrease in the electron population in the  $d_{x^2-y^2}$  states but by an increase in density of holes in the  $d_{z^2-x^2}$  and  $d_{z^2-y^2}$  states. Consequently, the electrons must predominantly occupy the corresponding orthogonal states, i.e.,  $d_{3x^2-r^2}$  and  $d_{3y^2-r^2}$ .

Although the Mn  $L$  spectra from manganites have been well studied there is still a lot of discussion and perhaps a lack of unanimity whether the two fine structure features of the  $L_3$  multiplet can be assigned to two different valence states of Mn ions in these systems [12, 18–27]. This, in other words, would mean that there are two distinct separable species of Mn ions in the lattice for which there is no experimental evidence except when one of them happens to come from a phase impurity [26]. In fact, this question has recently been systematically examined by Herrero-Martín *et al* [28] and they reach a conclusion against the presence of distinct  $\text{Mn}^{3+}/\text{Mn}^{4+}$

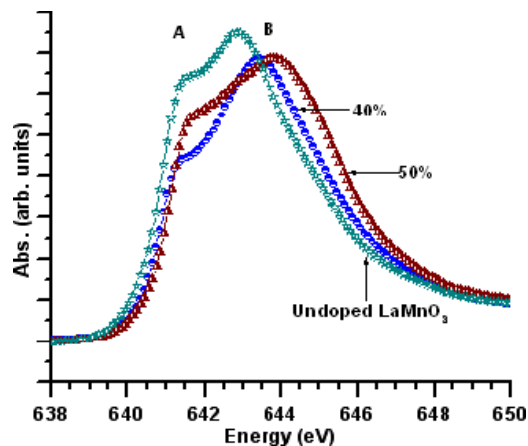


**Figure 5.** The  $E \parallel a$  polarized Mn  $L_3$  spectra for the cubic undoped  $\text{LaMnO}_3$ , the 40% doped  $\text{La}_{1.2}\text{Sr}_{1.65}\text{Ca}_{0.15}\text{Mn}_2\text{O}_7$ , and the 50% doped  $\text{LaSr}_2\text{Mn}_2\text{O}_7$  quasi-2D bilayer crystals. A and B respectively represent the low- and high-energy features of the Mn  $L_3$  multiplet.

integer valence states for any of their mixed-valence samples. The spectra for the cubic system  $\text{La}_{1-x}\text{Sr}_x\text{MnO}_3$  can be simulated, as shown by de Groot *et al* [24], by calculating the projection of the atomic multiplets in octahedral symmetry. It has recently been shown that even though the Mn 3d states are hybridized with O 2p orbitals, the Mn L spectra can also be reasonably simulated using atomic like theory taking into account the presence of 2p core holes [27]. This would imply that the d states are localized. However, in discussion of the O K spectrum earlier we have seen incontrovertible experimental evidence that points to hybridization of O 2p with the Mn 3d states. Such a hybridization is not possible if the Mn 3d states were localized. Mn 3d states may thus be speculated to be itinerant in nature, forming band states that hybridize with O 2p band. In fact, Wessely *et al* [27] have, on the basis of their experiment and calculations based on atomic like theory, argued how the electronic structure of doped manganites is perhaps best explained assuming an itinerant nature for the Mn 3d states in the ground state.

To conclude the Mn L and O K spectra do not provide any indication towards presence of the formal  $\text{Mn}^{4+}$  valence ions in the doped bilayer systems. Furthermore, it is found that the competition between the charge dynamics and the lattice distortion leads to transfer of some of the holes doped in the out-of-plane ( $3z^2 - r^2$ ) states to the in-plane ( $x^2 - y^2$ ) states. The changes observed in these with doping are shown not to be due to a decrease in the electron population in the  $d_{x^2-y^2}$  states but by an increase in density of holes in the  $d_{z^2-x^2}$  and  $d_{z^2-y^2}$  states and the electrons predominantly occupy the corresponding orthogonal states, i.e.,  $d_{3x^2-r^2}$  and  $d_{3y^2-r^2}$ . All in all, the changes observed in the spectra with polarization and with doping can be understood only if the Mn 3d states are speculated to be itinerant in nature.

## References

[1] Goodenough J B 2004 *Rep. Prog. Phys.* **67** 1915 and references therein

- Jin S *et al* 1994 *Science* **264** 413  
 Chahara K *et al* 1993 *Appl. Phys. Lett.* **63** 1990  
 von Helmholt R *et al* 1993 *Phys. Rev. Lett.* **71** 2331  
 Kusters R M *et al* 1989 *Physica B* **155** 362  
 [2] Millis A J *et al* 1995 *Phys. Rev. Lett.* **74** 5144  
 [3] Tokura Y (ed) 2000 *Colossal Magnetoresistive Oxides* (New York: Gordon and Breach)  
 Zener C 1951 *Phys. Rev.* **82** 403  
 Anderson P W and Hasegawa H 1955 *Phys. Rev.* **100** 675  
 de Gennes P G 1960 *Phys. Rev.* **118** 141  
 Nagaev E L 1995 *Phys.—Usp.* **38** 497 and references therein  
 Moreo A, Yunoki S and Dagotto E 1999 *Science* **283** 2034  
 [4] Moritomo Y *et al* 1996 *Nature* **380** 141  
 Kimura T *et al* 1996 *Science* **274** 1968  
 Mitchell J F *et al* 1997 *Phys. Rev. B* **55** 63  
 [5] Mitchell J F, Argyriou D N and Jorgensen J D 2000 *Colossal Magnetoresistive Oxides* ed Y Tokura (New York: Gordon and Breach) and references therein  
 [6] Kimura T, Kumai R, Tokura Y, Li J Q and Matsui Y 1998 *Phys. Rev. B* **58** 11 081  
 Li J Q, Matsui Y, Kimura T and Tokura Y 1998 *Phys. Rev. B* **57** R3205  
 [7] Goodenough J B 1955 *Phys. Rev.* **100** 564  
 [8] Argyriou D N, Bordallo H N, Campbell B J, Cheetham A K, Cox D E, Gardner J S, Hanif K, dos Santos A and Strouse G F 2000 *Phys. Rev. B* **61** 15 269  
 Radaelli P G, Cox D E, Marezio M and Cheong S-W 1997 *Phys. Rev. B* **55** 3015  
 Sternlieb B J, Hill J P, Wildgruber U C, Luke G M, Nachumi B, Moritomo Y and Tokura Y 1996 *Phys. Rev. Lett.* **76** 2169  
 [9] Akimoto T, Moritomo Y, Ohoyama K, Okamoto S, Ishihara S, Maekawa S and Nakamura A 1999 *Phys. Rev. B* **59** R14 153  
 [10] Mizokawa T and Fujimori A 1997 *Phys. Rev. B* **56** R493  
 [11] Takata M, Nishibori E, Kato K, Sakata M and Moritomo Y 1999 *J. Phys. Soc. Japan* **68** 2190  
 Zimmermann M v, Hill J P, Gibbs D, Blume M, Casa D, Keimer B, Murakami Y, Tomioka Y and Tokura Y 1999 *Phys. Rev. Lett.* **83** 4872  
 [12] Mitra C, Hu Z, Raychaudhari P, Wirth S, Csiszar S I, Hsieh H H, Lin H-J, Chen C T and Tjeng L H 2003 *Phys. Rev. B* **67** 92404  
 [13] Herrero-Martin J, Garcia J, Subias G, Blasco J and Sanchez M C 2005 *Phys. Rev. B* **72** 85106  
 [14] Sikora M, Kapusta Cz, Knížek K, Jiráček Z, Autret C, Borowiec M, Oates C J, Procházka V, Rybicki D and Zajac D 2006 *Phys. Rev. B* **73** 094426  
 [15] Velazquez M, Haut C, Hennion B and Revcolevschi A 2000 *J. Cryst. Growth* **220** 480  
 [16] Nannarone S, Borgatti F, DeLuisa A, Doyle B P, Gazzadi G C, Giglia A, Finetti P, Mahne N, Pasquali L, Pedio M, Selvaggi G, Naletto G, Pelizzo M G and Tondello G 2003 *Synchrotron Radiation Instrumentation: 8th Int. Conf. on Synchrotron Radiation Instrumentation (AIP Conf. Proc. No. 705)* ed T Warwick, J Stohr, H A Padmore and J Arthur (Melville, NY: AIP) pp 450–3  
 [17] Zangrando M, Finazzi M, Paolucci G, Comelli G, Diviacco B, Walker R P, Cocco D and Parmigiani F 2001 *Rev. Sci. Instrum.* **72** 1313  
 [18] Park J-H, Kimura T and Tokura Y 1998 *Phys. Rev. B* **58** R13330  
 [19] Merz M, Roth G, Reutler P, Buchner B, Arena D, Dvorak J, Idzerda Y U, Tokumitsu S and Schuppler S 2006 *Phys. Rev. B* **74** 184414  
 [20] Abbate M, de Groot F M F, Fuggle J C, Fujimori A, Strebel O, Lopez F, Domke M, Kaindl G, Sawatzky G A, Takano M,

- Takeda Y, Eisaki H and Uchida S 1992 *Phys. Rev. B* **46** 4511
- [21] Ibrahim K, Qian H J, Wu X, Abbas M I, Wang J O, Hong C H, Su R, Zhong J, Dong Y H, Wu Z Y, Wei L, Xian D C, Li Y X, Lapeyre G J, Mannella N, Fadley C S and Baba Y 2004 *Phys. Rev. B* **70** 224433
- [22] Sugano S, Tanabe Y and Kamimura H 1970 *Multiplets of Transition Metal Ions in Crystals* (New York: Academic)
- [23] Merz M, Reutler P, Buchner B, Arena D, Dvorak J, Idzerda Y U, Tokumitsu S and Schuppler S 2006 *Eur. Phys. J. B* **51** 315
- [24] de Groot F M F, Fuggle J C, Thole B T and Sawatzky G A 1990 *Phys. Rev. B* **41** 928
- de Groot F M F, Fuggle J C, Thole B T and Sawatzky G A 1990 *Phys. Rev. B* **42** 5457
- [25] Mitra C, Hu Z, Raychaudhuri P, Wirth S, Csiszar S I, Hsieh H H, Lin H-J, Chen C T and Tjeng L H 2003 *Phys. Rev. B* **67** 92404
- [26] de Jong M P, Bergenti I, Dediu V, Fahlman M, Marsi M and Taliani C 2005 *Phys. Rev. B* **71** 14434
- [27] Wessely O, Roy P, Åberg D, Andersson C, Edvardsson S, Karis O, Sanyal B, Svedlindh P, Katnelson M L, Gunnarsson R, Arvanitis D, Bengone O and Eriksson O 2006 *Phys. Rev. B* **68** 235109
- [28] Herrero-Martín J, García J, Subías G, Blasco J and Sánchez M C 2005 *Phys. Rev. B* **72** 85106